

A Supramolecular Capsule for Reversible Polysulfide Storage/Delivery in Lithium-Sulfur Batteries

Jin Xie[†], Hong-Jie Peng[†], Jia-Qi Huang, Wen-Tao Xu, Xiang Chen, and Qiang Zhang*

Abstract: Supramolecular materials, in which small organic molecules are assembled into regular structures by non-covalent interactions, attract tremendous interests because of their highly tunable functional groups and porous structure. Supramolecular adsorbents are expected to fully expose their abundant adsorptive sites in a dynamic framework. In this contribution, we introduced cucurbit[6]uril as a supramolecular capsule for reversible storage/delivery of mobile polysulfides in lithium-sulfur (Li-S) batteries to control undesirable polysulfide shuttle. The Li-S battery equipped with the supramolecular capsules retains a high Coulombic efficiency and shows a large increase in capacity from 300 to 900 mAh g⁻¹ at a sulfur loading of 4.2 mg cm⁻². The implementation of supramolecular capsules offers insights into intricate multi-electron-conversion reactions and manifests as an effective and efficient strategy to enhance Li-S batteries and analogous applications that involve complex transport phenomena and intermediate manipulation.

Supramolecular materials, in which small organic building blocks are regularly assembled into well-defined structures by non-covalent interactions, are fascinating for their integrated functional groups, adjustable spatial structures, and environmental benignity.^[1] Driven by diverse inter- and intramolecular interactions, the assembly of supramolecular materials play a vital role in not only organic chemistry but also material design toward a sustainable future through lots of cutting-edge applications like adaptive adsorption and smart energy storage. Aiming at energy storage, supramolecular materials have been employed directly as device components^[1b,2] or indirectly for synthesizing electrode materials.^[3] Owing to their superior chemical tunability, topological diversity, and dynamic adaptiveness, supramolecular materi-

als are especially promising to regulate complex transport phenomena and intermediate reactions, which are torturing some emerging chemistries such as lithium-sulfur (Li-S) batteries.

Li-S batteries, regarded as one of the most promising candidates for future energy storage, are attractive for extremely high energy density (theoretically 2600 Wh kg⁻¹ based on reaction: S + 2Li = Li₂S), low costs, and environmental friendliness.^[4] Unfortunately, Li-S batteries are suffering from problems including low sulfur utilization, self-discharge, low efficiency, and poor cycling stability. These issues are mainly originated from the shuttle effect that soluble intermediates, lithium polysulfides (LiPSs; Li₂S_x, x = 4–8), induce an internal redox cycle that lowers the charge efficiency and phase migration that accounts for loss of active materials.^[5] Hence, effectively immobilizing LiPSs is of paramount fundamental and practical significance for realizing reliable Li-S batteries.

To immobilize LiPSs in a working Li-S cell, one of the simplest yet efficient strategies is introducing LiPS adsorbents. A variety of polar adsorbents has been applied, including inorganics,^[6] heteroatom-doped carbon,^[7] and polymers.^[8] On one hand, inorganics are often dominated with exceptional affinity to LiPSs; however, the usually low specific area and high atomic weight restrict the specific adsorption capacity, and too high the binding energy is detrimental to reversible desorption or facile diffusion of LiPSs to conductive surface, restraining subsequent conversion.^[6,9] For instance, even very small (5 nm) and uniform inorganic particles can only afford less than 33% of surface atoms for adsorption. On the other hand, heteroatom-doped carbons, ideally single-layer doped graphene, possess fully exposed surface and moderate binding energies to LiPSs; while the adsorption ability is limited by insufficient content of adsorptive atoms.^[5c] An ideal adsorbent consequently requires several critical attributes: (1) modest affinity to LiPSs, (2) high density of adsorptive sites, (3) full accessibility to these sites, and (4) reversibility upon electrochemical reactions. These desirable attributes, fortunately, are fully met by rationally designed supramolecular materials, which is capable of efficiently and reversibly capturing/delivering LiPSs (Figure 1).

In this contribution, a prototype supramolecular material, cucurbituril (CB), was demonstrated as an efficient LiPS capsule for Li-S batteries. CBs are a class of macrocyclic amidals consisting of glycoluril (=C₄H₂N₄O₂=) monomers linked by methylene bridges. The CB capsule has numerous merits including 1) moderate affinities of Lewis basic binding sites (tertiary-N and carbonyl-O),^[10] 2) a large atomic fraction of these binding sites (33.3% of tertiary-N and 16.7% of carbonyl-O) in its backbone, 3) densely arranged and fully

[*] J. Xie,^[†] H.-J. Peng,^[†] X. Chen, Prof. Q. Zhang
Beijing Key Laboratory of Green Chemical Reaction
Engineering and Technology, Department of
Chemical Engineering, Tsinghua University
Beijing 100084 (PR China)
E-mail: zhang-qiang@mails.tsinghua.edu.cn
Prof. J.-Q. Huang
Advanced Research Institute of Multidisciplinary Science
Beijing Institute of Technology
Beijing 100081 (PR China)
W.-T. Xu
Department of Chemistry, University of California
Berkeley, CA 94720 (USA)

[†] These authors contributed equally to this work.

Supporting information and the ORCID identification number(s) for the author(s) of this article can be found under:
<https://doi.org/10.1002/anie.201710025>.

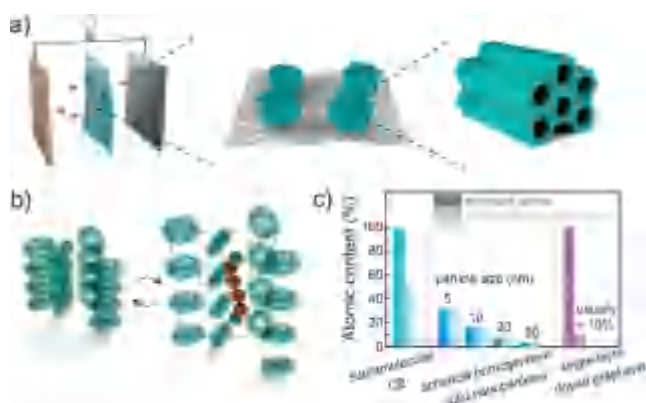


Figure 1. Conceptual illustration of supramolecular capsules. Schematics for a) a Li-S battery with a G@CB interlayer to reversibly trap LiPSs (left), CB capsules on graphene substrate (middle), and one-dimensional micropore channels in CB, and for b) the reversible storage/delivery process of LiPSs in adaptive CB channels. c) Comparison of exposure ratio of adsorptive atoms between different materials: CB (53% and 50% by weight and atom number, respectively; H atoms are neglected), spherical homogeneous particles without interior exposure ($\leq 33\%$ for 5-nm particles), and doped carbon (exemplified as ideal single-layer doped graphene) with an atomic doping level usually $< 10\%$.

exposed micropores in some polymorphs, and 4) dynamic H-bonded networks with extraordinary structural flexibility. All these merits render CB as a superior reservoir to reversibly store and deliver polysulfide guests, during which its framework structure dynamically changes to adapt to the adsorption/desorption. When delicately hybridized with conductive graphene (G@CB), a LiPS-breathable membrane was fabricated to suppress LiPS shuttle and improve their retention/utilization (Figure 1a). As a consequence, electrochemical performance of Li-S batteries employing a G@CB interlayer was enhanced significantly.

Among the CB family, the CB with six glycoluril units, that is, cucurbit[6]uril, has attracted the most interests because of its highest structural stability and strongest capability of forming a H-bonded supramolecular framework with aligned micropore channels of 6.0–7.5 Å (Figure 1a).^[11] Thus it was used for proof-of-concept, and in following contents, CB is mainly referred to cucurbit[6]uril. In addition to the tremendously higher atomic content of binding sites than that of doped graphene, CB possesses an exotic cage-like structure that favors two functions: on one hand, electronegative N and O atoms are mainly located at the edge, rendering electron-rich apertures to coordinate with electron-deficient guest molecules, e.g., LiPSs; on the other hand, the less electrified band facilitates the self-assembly of CB into an ordered supramolecular structure (see Figure S1 in the Supporting Information). Interactions between CB and various LiPSs were simulated through theoretical calculation, indicating moderate binding energies from -1.5 to -1.0 eV that benefit facile and reversible adsorption/desorption of LiPSs (Figure S2).

The interaction was further verified experimentally by using Li_2S_6 as a probe molecule and bulk supramolecular CB as the adsorbent (200–500 nm in diameter, Figure S3). The

Raman spectrum of CB after adsorbing LiPSs (CB- Li_2S_6), unlike that of LiPSs in dimethoxyethane (DME) solvent, exhibits vibration modes of only CB and Li_2S_6 but no signals of solvents, indicating that CB selectively extracted LiPSs from electrolyte (Figure 2a). Furthermore, it is observed that

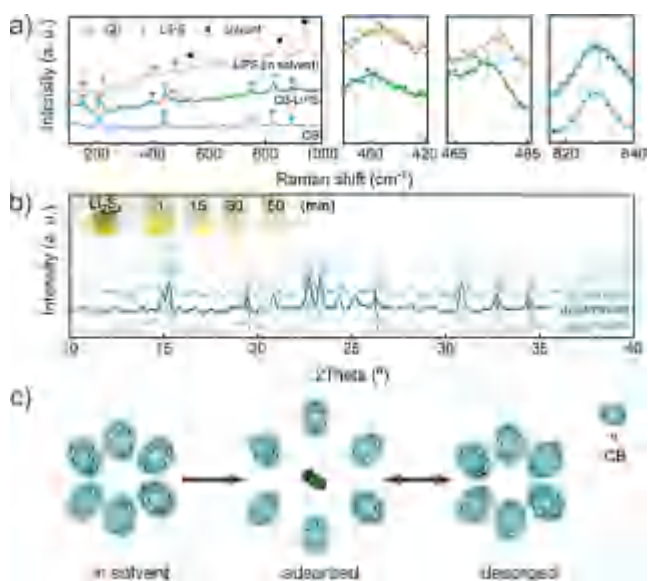


Figure 2. LiPS adsorption/desorption phenomena in CB. a) Raman spectra of CB- Li_2S_6 , pristine CB and dissolved Li_2S_6 in DME solvent. b) X-ray diffraction (XRD) patterns of pristine CB, CB swelled by DME, and CB after Li_2S_4 adsorption and desorption, as well as (inset) a digital picture showing the rapid adsorption process. c) Schematics for the “LiPS-breathing” model, showing the stretch and shrink of supramolecular framework during adsorption and desorption.

there are red shifts of 3.9 and 2.7 cm^{-1} for signals of Li_2S_6 (403.9 and 476.5 cm^{-1}) and a blue shift of 1.1 cm^{-1} for that of CB (828.6 cm^{-1}), respectively, in the spectrum of CB- Li_2S_6 with respect to spectra of pure CB and Li_2S_6 (in solvent). The red shifts correspond to reduced force constants of S–S and S–Li bonds within LiPSs, possibly due to Li–O interactions endowed by CB; while the blue shift is ascribed to the positive stress induced by aforementioned interactions. Such interactions were further validated by X-ray photoelectron spectroscopy (Figure S4). The effective CB- Li_2S_6 interactions probed spectroscopically fully agrees with theoretical simulation.

Aside from the atomic interactions, the interplay between CB and LiPSs also manifests as an abnormal adsorptive behavior. As N_2 isotherm indicated, the bulk crystal of supramolecular CB is featured with a dominant 7-Å micropore (Figure S5). Such a pore size should have been too small to allow a solvated LiPS molecule (ca. 8 Å) in.^[12] Nevertheless, even bulk CB crystals embodied outstanding adsorptivities to LiPSs (herein Li_2S_4), showing a larger mass adsorption capacity than graphene (Figure S6) and a rapid adsorption kinetics (inset of Figure 2b).

Such an abnormal adsorptive behavior of CB implies a unique underlying mechanism. To disclose it, changes in the bulk structure of CB during LiPS adsorption/desorption were analyzed by ex-situ XRD (Figure 2b). The XRD pattern of

pristine CB is in good accordance with a supramolecular crystal form suggested previously.^[11] Once being swelled by DME or adsorbing LiPSs, the crystal lattice of CB suffered from a notable expansion, as indicated by the XRD peak shifts. The dynamic stretching of CB framework is attributed to the filling of micropore channels by solvent and/or Li₂S₄ molecules sequentially. The expansion ratios from CB to CB-Li₂S₄ are in range of 0.20–0.83%, varying with the peak position, namely the crystal orientation (Table S1). Such an asynchronous nature reveals the anisotropic expansion of CB upon LiPS adsorption, which originates from the structural alterability of supramolecular assemblies. Besides these shifts, signal of impurities, that is, crystalline LiPSs and their decomposing products such as sulfur and Li₂S, cannot be detected.

The inverse process was further modeled by treating the CB-Li₂S₄ with a large amount of DME to strip the adsorbed LiPSs out. The pristine CB crystal form was well restored as all peaks shifted back to the original positions (Figure 2b). This indicates the excellent reversibility of adsorption/desorption processes, making CB a very promising LiPS capsule.

All above phenomena and evidences suggest 1) the well maintenance of supramolecular structure, 2) the encapsulation of LiPSs, instead of other crystalline sulfur species, in micropore channels, and 3) the dynamic expansion and restoration of CB framework (Figure 2c). The desirable structural alterations are attributed to the inherent adaptiveness of CB supramolecular framework linked by dynamic H-bonds.

To make full use of the efficient and reversible LiPS storage/delivery, CB was engineered as nanoparticles deposited on graphene, forming a LiPS-breathable G@CB membrane (Figure S7). Graphene was introduced to serve as 1) a highly conductive substrate and 2) a soft template to guide the growth of CB nanoparticles. The G@CB membrane exhibits an interconnected porous scaffold, in which each sheet has a lateral size of 5–20 μm (Figure 3a). A monolayer of CB is

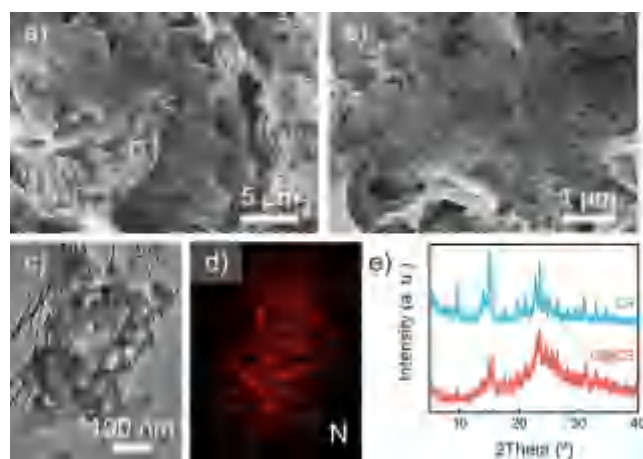


Figure 3. Morphological characterization of G@CB interlayer. a, b) Scanning electron microscopy and c) transmission electron microscopy images, as well as d) corresponding energy dispersive spectroscopy mapping of G@CB. e) XRD patterns of CB and G@CB.

found to be firmly attached, forming a thin, conformal, and porous coating on a single graphene sheet (Figure 3b). Its thinness and porous nature contribute to short ion diffusion lengths and ease the access of LiPSs to each CB capsules. Primary CB particles possess an average radius of around 15 nm, significantly smaller than the bulk CB particles (Figure 3c). Elemental mapping confirms the uniformity of CB coating (Figure 3d). The reduced grain size of CB on graphene is also revealed by dramatically weakened and broadened XRD peaks (Figure 3e). The small size of as-obtained CB nanoparticles has hardly been realized. These attributes are believed to be very promising for efficient and reversible storage/delivery of certain guest molecules like LiPSs.

G@CB was coated on polypropylene (PP) separators with an areal loading of 0.1 mg cm⁻¹ and an average thickness of 4 μm (Figure S8). As demonstrated above, such a thin and light G@CB coating is able to trap LiPSs when they are vigorously dissolved and deliver adsorbed LiPSs when free LiPSs are consumed out during reactions. This scenario is realized through the unique adsorption/desorption behaviors of LiPSs in dynamic and adaptive CB framework, which somewhat ensemble to other counterintuitive adsorption phenomena.^[13]

By employing replacing a G@CB-coated separator to replace the PP membrane, the initial specific capacity of a Li-S cell was improved from 893 to 1032 mAh g⁻¹ at a current density of 0.5 C (1 C = 1672 mA g⁻¹), when a blended sulfur/carbon cathode (sulfur content: 63 wt.%; sulfur loading: 1.0 mg cm⁻²) was employed (Figure 4a). After 300 cycles, a capacity of 678 mAh g⁻¹ was preserved for the cell with a G@CB-coated separator. More importantly, a high Coulombic efficiency (CE) of 92% was maintained. In contrast, the controlled cell with a PP separator exhibited continuous decay of CE to 87% until around 160 cycles; after that, CE sharply decrease to lower than 80%, in accordance with cell failure. The origin of cell failure was further implied by the

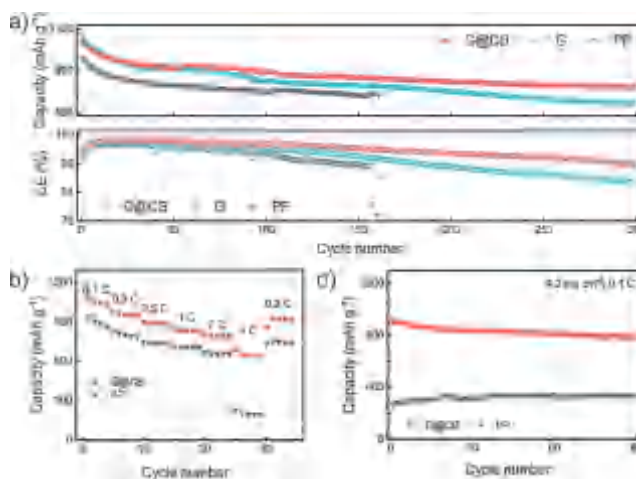


Figure 4. Electrochemical performances. a) Cycling performance at a current density of 0.5 C, regarding the capacity (upper) and CE (bottom), and b) rate performance of Li-S cells (sulfur loading: 1.0 mg cm⁻²). c) Cycling performance of high-loading Li-S cells (sulfur loading: 4.2 mg cm⁻²) at a current density of 0.1 C.

sudden drop of voltage and severe overcharge in charge profiles (Figure S9). Due to the rampant LiPS shuttle in control cell, the lithium metal anode was out of protection, leading to dendrite growth and short circuit.

To illustrate the pivotal role of supramolecular CB capsules, graphene (G)-coated separators were fabricated for comparison. A comparable initial capacity to that in case of G@CB was realized; however, the capacity fading was much faster. Especially after around 160 cycles, both the capacity and CE decays were accelerated with only 563 mAhg⁻¹ and 87% preserved after 300 cycles, 17 and 5.4% lower than those of the cell with G@CB, respectively. It is interesting to find that capacity fading is strongly correlated to CE retention in this case, further indicating the role of CB in retarding the LiPS shuttle.

Despite the use of LiNO₃ that protects lithium metal from LiPS corrosion, LiNO₃ suffers from continuous consumption. The exhaustion of LiNO₃ accounted for the sudden death of routine Li-S cell employing a PP separator. G-coated separator improved the initial utilization; but after long-term cycling, the CE still decayed continuously, suggesting the limited role of graphene. Only G@CB with abundant supramolecular nanocapsules incorporated was capable of restraining shuttle and sustaining considerable utilization of sulfur. The promotion effect of CB was also validated by engineering either a CB or a physically mixed G/CB coating layer on the separator, which enhanced CE even without LiNO₃ (Figures S10 and S11). But the G@CB-coated one is among the best due to the delicate design and good structural integrity after cycling (Figure S12).

The cooperation of CB capsule and graphene is anticipated to accelerate the adsorption and conversion of LiPSs at G@CB interface, leading to enhanced rate performance (Figure 4b). A high capacity of 1084 mAhg⁻¹ was achieved at 0.1 C with the G@CB interlayer, and when further increasing the current rate to 0.2, 0.5, 1.0, and 2.0 C, the capacity reached 978, 898, 848, and 799 mAhg⁻¹, respectively, much higher than the controlled cell. Even at a high rate of 4.0 C, the cell with G@CB maintained a tenacious capacity of 691 mAhg⁻¹. In contrast, the discharge capacity in the absence of G@CB dropped sharply to 229 mAhg⁻¹ when the rate doubled from 2.0 C to 4.0 C. The enhanced rate performance indicated the promoted kinetics.

To further excavate the practicality of G@CB-coated separators, high-loading cathode (sulfur loading: 4.2 mgcm⁻²) was employed. The discharge capacity of modified Li-S cell with a G@CB separator was initially 900 mAhg⁻¹ and kept 800 mAhg⁻¹ for almost 90 cycles at 0.1 C. However, the battery with a PP separator only exhibited capacities of less than 400 mAhg⁻¹, incomparable to even half of that delivered by the modified Li-S cell. Note that G@CB layer (0.2 mgcm⁻²) only accounts for 2.9 wt% of the whole cathode, which is almost negligible compared to the performance enhancement. The enhancement in both capacity and cycling stability is notably valuable for practical applications and comparable or even better than previous studies employing functional separators/interlayers (Table S2).^[6e,14]

The above enhancement is attributed to rational material selection and structural design of G@CB, which possesses

following advantages: 1) moderate affinities to reversibly immobilize LiPSs, 2) high adsorption capacity owing to the largely exposed and high-density adsorptive sites, 3) high storage/delivery flux passing through the CB nanocapsules, and 4) short ion diffusion length between adsorption sites and conductive surface. Consequently, the favorable thermodynamic adsorptivity and rapid kinetic diffusion are integrated and synergistically embodied in Li-S cells with a high sulfur areal loading and operated at high current rates. More importantly, unlike previous reports, in which supramolecular materials were used as cathode coating^[15] or redox mediator,^[16] CB capsules herein exhibit a counterintuitive adsorptive behavior to adaptively store and release LiPSs. We are especially interested in the unknown role of a dynamic framework in guest-molecule-involving energy storage devices like Li-S batteries and attempt to unravel the underlying working mechanism. Hopefully the understanding and principle unveiled for these abnormal adsorptive phenomena will enlighten the future conceptual advancements.

In conclusion, a supramolecular capsule was proposed for LiPS storage/delivery in a working Li-S battery. Supramolecular CB with abundant exposed adsorptive sites rendered a large adsorption capacity to LiPSs. CB nanocapsules of 15 nm in radius were deposited on graphene to achieve fast kinetics. Consequently, the LiPS shuttle in Li-S cell was restrained, leading to enhanced capacity, cycling stability, and CE, even when high sulfur loading or high rates were applied. This contribution sheds fresh light on the exploration of functional supramolecular materials and brings new insights and ideas to the material selection and structure design for advanced Li-S batteries and analogues applications.

Acknowledgements

This work was supported by National Key Research and Development Program (2016YFA0202500 and 2016YFA0200102) and National Natural Science Foundation of China (21422604 and 21676160). The authors acknowledged the support from Tsinghua National Laboratory for Information Science and Technology for theoretical simulations.

Conflict of interest

The authors declare no conflict of interest.

Keywords: adsorption · cucurbituril · lithium–sulfur batteries · polysulfides · supramolecular chemistry

How to cite: *Angew. Chem. Int. Ed.* **2017**, *56*, 16223–16227
Angew. Chem. **2017**, *129*, 16441–16445

- [1] a) K. S. Mali, N. Pearce, S. De Feyter, N. R. Champness, *Chem. Soc. Rev.* **2017**, *46*, 2520–2542; b) N. M. Sangeetha, U. Maitra, *Chem. Soc. Rev.* **2005**, *34*, 821–836.
- [2] a) J. H. Lee, J. Park, J. W. Park, H. J. Ahn, J. Jaworski, J. H. Jung, *Nat. Commun.* **2015**, *6*, 6650; b) C. Wang, H. Wu, Z. Chen, M. T. McDowell, Y. Cui, Z. N. Bao, *Nat. Chem.* **2013**, *5*, 1042–1048;

- c) G. Y. Zheng, C. Wang, A. Pei, J. Lopez, F. F. Shi, Z. Chen, A. D. Sendek, H. W. Lee, Z. D. Lu, H. Schneider, M. M. Safont-Sempere, S. Chu, Z. N. Bao, Y. Cui, *ACS Energy Lett.* **2016**, *1*, 1247–1255.
- [3] W. Ai, J. Jiang, J. H. Zhu, Z. X. Fan, Y. L. Wang, H. Zhang, W. Huang, T. Yu, *Adv. Energy Mater.* **2015**, *5*, 1500559.
- [4] a) R. Fang, S. Zhao, Z. Sun, D. W. Wang, H. M. Cheng, F. Li, *Adv. Mater.* **2017**, *29*, 1606823; b) A. Manthiram, S. H. Chung, C. X. Zu, *Adv. Mater.* **2015**, *27*, 1980–2006.
- [5] a) H. J. Peng, J. Q. Huang, X. B. Cheng, Q. Zhang, *Adv. Energy Mater.* **2017**, *7*, 1700260; b) L. Borchardt, M. Oschatz, S. Kaskel, *Chem. Eur. J.* **2016**, *22*, 7324–7351; c) Q. Pang, X. Liang, C. Y. Kwok, L. F. Nazar, *Nat. Energy* **2016**, *1*, 16132.
- [6] a) X. L. Ji, S. Evers, R. Black, L. F. Nazar, *Nat. Commun.* **2011**, *2*, 325; b) R. Demir-Cakan, M. Morcrette, F. Nouar, C. Davoisne, T. Devic, D. Gonbeau, R. Dominko, C. Serre, G. Ferey, J. M. Tarascon, *J. Am. Chem. Soc.* **2011**, *133*, 16154–16160; c) S. Evers, T. Yim, L. F. Nazar, *J. Phys. Chem. C* **2012**, *116*, 19653–19658; d) J. M. Zheng, J. Tian, D. X. Wu, M. Gu, W. Xu, C. M. Wang, F. Gao, M. H. Engelhard, J. G. Zhang, J. Liu, J. Xiao, *Nano Lett.* **2014**, *14*, 2345–2352; e) Z. B. Xiao, Z. Yang, L. Wang, H. G. Nie, M. E. Zhong, Q. Q. Lai, X. J. Xu, L. J. Zhang, S. M. Huang, *Adv. Mater.* **2015**, *27*, 2891–2898; f) X. Y. Tao, J. G. Wang, C. Liu, H. T. Wang, H. B. Yao, G. Y. Zheng, Z. W. Seh, Q. X. Cai, W. Y. Li, G. M. Zhou, C. X. Zu, Y. Cui, *Nat. Commun.* **2016**, *7*, 11203.
- [7] a) L. W. Ji, M. M. Rao, H. M. Zheng, L. Zhang, Y. C. Li, W. H. Duan, J. H. Guo, E. J. Cairns, Y. G. Zhang, *J. Am. Chem. Soc.* **2011**, *133*, 18522–18525; b) J. X. Song, M. L. Gordin, T. Xu, S. R. Chen, Z. X. Yu, H. Sohn, J. Lu, Y. Ren, Y. H. Duan, D. H. Wang, *Angew. Chem. Int. Ed.* **2015**, *54*, 4325–4329; *Angew. Chem.* **2015**, *127*, 4399–4403; c) G. M. Zhou, E. Paek, G. S. Hwang, A. Manthiram, *Nat. Commun.* **2015**, *6*, 7760; d) J. J. Chen, R. M. Yuan, J. M. Feng, Q. Zhang, J. X. Huang, G. Fu, M. S. Zheng, B. Ren, Q. F. Dong, *Chem. Mater.* **2015**, *27*, 2048–2055.
- [8] a) L. F. Xiao, Y. L. Cao, J. Xiao, B. Schwenzer, M. H. Engelhard, L. V. Saraf, Z. M. Nie, G. J. Exarhos, J. Liu, *Adv. Mater.* **2012**, *24*, 1176–1181; b) Z. W. Seh, Q. F. Zhang, W. Y. Li, G. Y. Zheng, H. B. Yao, Y. Cui, *Chem. Sci.* **2013**, *4*, 3673–3677; c) C. Y. Chen, H. J. Peng, T. Z. Hou, P. Y. Zhai, B. Q. Li, C. Tang, W. C. Zhu, J. Q. Huang, Q. Zhang, *Adv. Mater.* **2017**, *29*, 1606802.
- [9] H. J. Peng, G. Zhang, X. Chen, Z. W. Zhang, W. T. Xu, J. Q. Huang, Q. Zhang, *Angew. Chem. Int. Ed.* **2016**, *55*, 12990–12995; *Angew. Chem.* **2016**, *128*, 13184–13189.
- [10] a) T. Z. Hou, X. Chen, H. J. Peng, J. Q. Huang, B. Q. Li, Q. Zhang, B. Li, *Small* **2016**, *12*, 3283–3291; b) T. Z. Hou, W. T. Xu, X. Chen, H. J. Peng, J. Q. Huang, Q. Zhang, *Angew. Chem. Int. Ed.* **2017**, *56*, 8178–8182; *Angew. Chem.* **2017**, *129*, 8290–8294.
- [11] a) S. Lim, H. Kim, N. Selvapalam, K. J. Kim, S. J. Cho, G. Seo, K. Kim, *Angew. Chem. Int. Ed.* **2008**, *47*, 3352–3355; *Angew. Chem.* **2008**, *120*, 3400–3403; b) H. Kim, Y. Kim, M. Yoon, S. Linn, S. M. Park, G. Seo, K. Kim, *J. Am. Chem. Soc.* **2010**, *132*, 12200–12202.
- [12] C. Y. Li, A. L. Ward, S. E. Doris, T. A. Pascal, D. Prendergast, B. A. Helms, *Nano Lett.* **2015**, *15*, 5724–5729.
- [13] S. Krause, V. Bon, I. Senkowska, U. Stoeck, D. Wallacher, D. M. Tobbens, S. Zander, R. S. Pillai, G. Maurin, F. X. Coudert, S. Kaskel, *Nature* **2016**, *532*, 348–352.
- [14] a) L. Kong, H. J. Peng, J. Q. Huang, W. C. Zhu, G. Zhang, Z. W. Zhang, P. Y. Zhai, P. Sun, J. Xie, Q. Zhang, *Energy Storage Mater.* **2017**, *8*, 153–160; b) J. Q. Huang, T. Z. Zhuang, Q. Zhang, H. J. Peng, C. M. Chen, F. Wei, *ACS Nano* **2015**, *9*, 3002–3011; c) H. J. Peng, Z. W. Zhang, J. Q. Huang, G. Zhang, J. Xie, W. T. Xu, J. L. Shi, X. Chen, X. B. Cheng, Q. Zhang, *Adv. Mater.* **2016**, *28*, 9551–9558; d) H. J. Peng, D. W. Wang, J. Q. Huang, X. B. Cheng, Z. Yuan, F. Wei, Q. Zhang, *Adv. Sci.* **2016**, *3*, 1500268; e) J. Balach, H. K. Singh, S. Gomoll, T. Jaumann, M. Klose, S. Oswald, M. Richter, J. Eckert, L. Giebeler, *ACS Appl. Mater. Interfaces* **2016**, *8*, 14586–14595; f) S. Y. Bai, X. Z. Liu, K. Zhu, S. C. Wu, H. S. Zhou, *Nat. Energy* **2016**, *1*, 16094; g) H. B. Yao, K. Yan, W. Y. Li, G. Y. Zheng, D. S. Kong, Z. W. Seh, V. K. Narasimhan, Z. Liang, Y. Cui, *Energy Environ. Sci.* **2014**, *7*, 3381–3390; h) S. H. Chung, A. Manthiram, *J. Phys. Chem. Lett.* **2014**, *5*, 1978–1983; i) T. Yim, S. H. Han, N. H. Park, M. S. Park, J. H. Lee, J. Shin, J. W. Choi, Y. Jung, Y. N. Jo, J. S. Yu, K. J. Kim, *Adv. Funct. Mater.* **2016**, *26*, 7817–7823; j) G. M. Zhou, S. F. Pei, L. Li, D. W. Wang, S. G. Wang, K. Huang, L. C. Yin, F. Li, H. M. Cheng, *Adv. Mater.* **2014**, *26*, 625–631.
- [15] C. B. Bucur, J. Muldoon, A. Lita, *Energy Environ. Sci.* **2016**, *9*, 992–998.
- [16] P. D. Frischmann, L. C. H. Gerber, S. E. Doris, E. Y. Tsai, F. Y. Fan, X. H. Qu, A. Jain, K. A. Persson, Y. M. Chiang, B. A. Helms, *Chem. Mater.* **2015**, *27*, 6765–6770.

Manuscript received: September 27, 2017

Accepted manuscript online: November 7, 2017

Version of record online: November 20, 2017